Science of the Total Environment 523 (2015) 40–49

Contents lists available at ScienceDirect

Science of the Total Environment

journal homepage: www.elsevier.com/locate/scitotenv

Adsorption of phosphate from aqueous solutions and sewage using zirconium loaded okara (ZLO): Fixed-bed column study

T.A.H. Nguyen [a], H.H. Ngo [a,*], W.S. Guo [a], T.Q. Pham [b], F.M. Li [c], T.V. Nguyen [a], X.T. Bui [d,e]

[a] Centre for Technology in Water and Wastewater, School of Civil and Environmental Engineering, University of Technology, Sydney (UTS), 15 Broadway, Ultimo, NSW 2007, Australia
[b] Faculty of Geography, University of Science, Vietnam National University, Hanoi, Viet Nam
[c] College of Environmental Science and Engineering, Ocean University of China, Qingdao 266100, China
[d] Environmental Engineering and Management Research Group, Ton Duc Thang University, Ho Chi Minh City, Viet Nam
[e] Faculty of Environment and Natural Resources, Ho Chi Minh City University of Technology-Vietnam National University, Ho Chi Minh City, Viet Nam

HIGHLIGHTS

- Dynamic adsorption of P from water and wastewater by Zr(IV)-loaded okara was tested.
- Effects of column design parameters on the adsorption performance were investigated.
- The dynamic adsorption capacity of Zr(IV)-loaded okara for P was reasonably high.
- The spent column was effectively regenerated with 0.2 M NaOH followed by 0.1 M HCl.
- Zr(IV)-loaded okara column was efficient in eliminating P from municipal sewage.

ARTICLE INFO

Article history:
Received 15 March 2015
Received in revised form 29 March 2015
Accepted 29 March 2015
Available online 7 April 2015

Editor: D. Barcelo

Keywords:
Phosphorus adsorption
Fixed-bed column
Zr(IV)-loaded okara
Soybean by-product (okara)
Food waste recycling
Agricultural by-products

ABSTRACT

This study explores the potential of removing phosphorus from aqueous solutions and sewage by Zr(IV)-loaded okara (ZLO) in the fixed-bed column. Soybean residue (okara) was impregnated with 0.25 M Zr(IV) solution to prepare active binding sites for phosphate. The effect of several factors, including flow rate, bed height, initial phosphorus concentration, pH and adsorbent particle size on the performance of ZLO was examined. The maximum dynamic adsorption capacity of ZLO for phosphorus was estimated to be 16.43 mg/g. Breakthrough curve modeling indicated that Adams–Bohart model and Thomas model fitted the experimental data better than Yoon–Nelson model. After treatment with ZLO packed bed column, the effluent could meet the discharge standard for phosphorus in Australia. Successful desorption and regeneration were achieved with 0.2 NaOH and 0.1 HCl, respectively. The results prove that ZLO can be used as a promising phosphorus adsorbent in the dynamic adsorption system.

1. Introduction

Phosphorus is not only an essential macro nutrient of living organisms and a fundamental material of many industries but also one of the major environmental concerns (Awual and Jyo, 2011). It is well-recognized that the phosphorus concentration in receiving water medium above 0.02 mg/L can cause eutrophication (Mallampati and Valiyaveettil, 2013). To protect surface water from this undesirable phenomenon, many countries have regulated the effluent discharge standard for total phosphorus, which varies from 0.5 to 1 mg/L at the most stringent. Thus, the elimination of phosphorus from effluents before discharging into aquatic medium is mandatory (Kalmykova and Fedje, 2013). The removal of phosphorus from water and wastewater can be achieved with several methods, such as membrane filtration, reverse osmosis (Greenlee et al., 2009), coagulation, precipitation, crystallization (Ackerman, 2012; Jia, 2014), adsorption/ion exchange (Biswas, 2008; Nur et al., 2014; Okochi, 2013), magnetic separation, biological treatment, and constructed wetland (Martín et al., 2013). Of these, adsorption is considered as an attractive option, owing to its simple operation, low cost, steady phosphorus removal, and potential for phosphorus recovery (Zhang et al., 2014).

Recently, there is a growing trend in using low-cost adsorbents for phosphorus elimination to reduce the cost of water treatment. In this context, several agricultural by-products have been tested as phosphorus

* Corresponding author at: School of Civil and Environmental Engineering, University of Technology, Sydney (UTS), P.O. Box 123, Broadway, NSW 2007, Australia.
E-mail address: ngohuuhao121@gmail.com (H.H. Ngo).

http://dx.doi.org/10.1016/j.scitotenv.2015.03.126
0048-9697/

adsorbents, e.g., apple peels, orange waste gel, bagasse, coir pith, and wood particles (Mallampati and Valiyaveettil, 2013; Biswas, 2008; Carvalho et al., 2011; Krishnan and Haridas, 2008; Eberhardt and Min, 2008). However, the biomaterials derived adsorbents often suffer from lack of mechanical strength, inefficiency in column adsorption with high flow rate, and limited reusability (Awual and Jyo, 2011). Although many studies have employed agricultural by-products as phosphorus adsorbents, very few reports have dealt with their application in real wastewater under continuous adsorption conditions (Bottini and Rizzo, 2012; Paudyal et al., 2013). The dynamic adsorption systems have significant advantages, such as treating large volume of wastewater, easy scale-up from lab-scale processes, simple operation, and reduced requirement of adsorbents (Kumar et al., 2011; Long et al., 2014). Thus, there is a need to perform continuous adsorption studies. The proper use of agricultural by-products as phosphorus adsorbents usually requires modification (e.g., metal loading, quaternization, thermal treatment) (Nguyen et al., 2014a). Metal loading provides the bio-materials with positively charged metal ions, which are suitable for retention of negatively charged anions, such as phosphate (Mallampati and Valiyaveettil, 2013). Zirconium was found to be an excellent loading metal in many studies performed by Biswas (2008); Mallampati and Valiyaveettil (2013); Nguyen et al., 2014b; Ohura et al. (2011), etc. However, the high-cost remains a challenge, limiting the use of zirconium compounds for this purpose (Nguyen et al., 2014c; Ren et al., 2012).

Soybean residue (okara) is considered as a potential material for the development of phosphorus adsorbent, due to the abundant availability, low cost, simple processing, and unique physical characteristics. A vast amount of okara is generated worldwide, especially in Asian countries. Though okara can be used for other purposes, it usually causes environmental burden due to the fast decay. Therefore, the utilization of okara for water treatment not only helps dispose of okara in a green way but also add value to this agricultural by-product. The idea of developing ZLO into phosphorus adsorbent is based on the formation of active binding sites for anions by loading okara with Zr(IV) solution. In the previous batch study, ZLO was proven to be a promising phosphorus adsorbent, due to high efficiency, selectivity and reusability (Nguyen et al., 2014c).

As the next step, the adsorption tests have been performed in the column mode with both synthetic solution and municipal sewage to evaluate the applicability of ZLO. It is expected to bring the adsorbent closer to industrial application, which is still the "bottleneck" of the adsorption technology. The previous studies on phosphate adsorption using agricultural by-products mainly focused on the potential but often paid no attention to the challenges to the process. However, in this study, the side effects of employing agricultural by-products derived phosphate adsorbents have been openly discussed. The specific objectives of this study are (1) to investigate the effect of process parameters and determine the dynamic adsorption capacity of ZLO, (2) to apply mathematical models including Bohart–Adams, Thomas, Yoon–Nelson, and BDST in describing experimental data, (3) to assess the applicability of ZLO in treating the sewage, and (4) to examine the reusability of ZLO.

2. Materials and methods

2.1. Chemicals and instruments

All chemical reagents used in this study were of analytical grade. Stock solution of phosphorus (1000 mg/L) was prepared by dissolving 4.58 g of disodium hydrogen phosphate (Na_2HPO_4) in a 1000 mL of milli-Q water. The pH of the solution was adjusted using NaOH or HCl solutions of different concentrations to ensure a minimal change in the volume of the solution. To prepare 0.05 M and 0.2 M NaOH solutions, 2 and 8 g of sodium hydroxide (NaOH) were dissolved in 1000 mL of milli-Q water, respectively. 80.56 g of zirconyl chloride octahydrate ($ZrOCl_2 \cdot 8H_2O$) was dissolved in 1000 mL of milli-Q water to produce 0.25 M Zr(IV) solution.

The concentration of phosphorus, nitrate, nitrite, and ammonium was measured using Spectroquant® NOVA 60 machine, whereas that of Zr(IV) and other metal ions was monitored using Microwave Plasma-Atomic Emission Spectrometer-Agilent Technologies 4100 MP-AES. The analysis of chloride and sulfate was performed using 790 Personal IC-Metrohm USA. The determination of total organic carbon (TOC) was conducted using Analytik Jena Multi C/N 3100.

2.2. Preparation of adsorbent

To develop a phosphorus adsorbent, this study employed soybean residue (hereinafter referred to as okara) as the substrate and zirconium as a loading metal. Okara was collected from Nhu Quynh tofu and soy milk workshop, Yagoona, NSW, Australia. In order to keep it for a long time, fresh okara was first dried at 105 °C for 24 h. Next, dried okara was pre-treated with 0.05 M NaOH at a solid/liquid ratio of 1:20, room temperature, 120 rpm for 24 h, followed by washing with distilled water and drying at 105 °C for 24 h again. Then, the dried NaOH pre-treated okara was impregnated in 0.25 M $ZrOCl_2 \cdot 8H_2O$ solution at the same conditions as above. This procedure led to the zirconium deposition onto okara (Mallampati and Valiyaveettil, 2013). Finally, ZLO of the desired particle size was obtained by sieving, kept in glass bottles and used for next experiments.

2.3. Experimental methods

2.3.1. Adsorption tests with synthetic solution

The column adsorption tests were conducted in glass mini-columns of 120 cm height and 1.75 cm inner diameter. To begin with, ZLO was stirred thoroughly with distilled water to enable the swelling and removing air bubbles. In the next step, it was packed into a column using the "slurry method" (Zach-Maor et al., 2011). The column was first filled with glass beads (~11 cm) at the bottom to produce an even flow. It was then packed with wet ZLO, followed by another layer of glass beads (~11 cm) and a piece of sponge to prevent ZLO from seeping out with the effluent. A certain amount of ZLO (5, 10, 15 g) was packed into the column to achieve the desired bed height (11.5, 23 and 34.5 cm). The feed solution containing various phosphorus concentrations (5.5, 10.2, and 15.5 mg/L), was pumped upward through the column at different flow rates (12, 20, and 28 mL/min) by peristaltic pumps. Effluent samples were collected at definite intervals of time in 14 mL plastic tubes for determination of the phosphorus concentration.

2.3.2. Application of ZLO in treating real municipal wastewater

The ability of ZLO packed bed column for phosphorus adsorption from sewage was evaluated with the same mini-column as above. Municipal wastewater secondary effluent was collected from Sydney Olympic Park Water Treatment Plant. Prior to the adsorption test, the sewage was settled for 24 h, filtered using a 150 μm sieve, and used for column adsorption tests without any pH alterations. The sewage was percolated into the column from bottom at the flow rate of 12 mL/min. The concentrations of phosphorus and major quality parameters of the solutions before and after passing through the column were determined according to standard procedures.

2.3.3. Desorption and regeneration tests with real municipal wastewater

Desorption and regeneration were performed with the same mini-columns as in adsorption. 0.2 M NaOH was chosen as desorption solution while 0.1 M HCl was used for regeneration since these solutions were proven to be effective in the previous batch experiments (Nguyen et al., 2014b). Prior to desorption, phosphorus loaded ZLO was rinsed with 300 mL distilled water at the flow rate of 12 mL/min to remove residual phosphorus. Then, 0.2 M NaOH solution was pumped upward through the column at flow rate of 12 mL/min until the phosphorus concentration of the effluent reached 5 mg/L. The desorbed ZLO column was washed with 1000 mL of distilled water at a flow rate of 36 mL/min. Then it was

reactivated with 1000 mL of 0.1 M HCl at a flow rate of 12 mL/min. After that, it was washed with 1000 mL of distilled water at a flow rate of 36 mL/min. The regenerated ZLO column was reused for the next cycle of adsorption–desorption. Three cycles have been implemented successively. Fig. 1 presented the schematic diagram of mini-column tests.

2.4. Calculation of breakthrough curve parameters

To evaluate the adsorption performance of a column, it is necessary to analyze the breakthrough curve. It can be done by calculating breakthrough curve parameters.

The breakthrough time (t_b) and treated volume at breakthrough time (V_b) are determined as the time and volume when the outlet phosphorus concentration (C_t) reached 10% of the inlet phosphorus concentration ($C_t/C_o = 0.1$). Similarly, the exhaustion time (t_s) and treated volume at exhaustion time (V_s) are defined as the time and volume when the outlet phosphorus concentration (C_t) reached 90% of the inlet phosphorus concentration ($C_t/C_o = 0.9$).

The total amount of phosphorus adsorbed onto ZLO column, q_{total} (mg) and the dynamic adsorption capacity, q_e (mg/g) are calculated according to the following equations (Paudyal et al., 2013):

$$q_{total} = \frac{Q}{1000} \int_{t=0}^{t=total} C_{ad}\,dt \quad (1)$$

$$q_e = \frac{q_{total}}{M} \quad (2)$$

where, t_{total}, Q, M, and C_{ad} are the total time for the column to reach saturation (min), volumetric flow rate (mL/min), the amount of ZLO packed in the column (g), and the difference in the phosphorus concentration at the initial time and the t time caused by adsorption (mg/L), respectively.

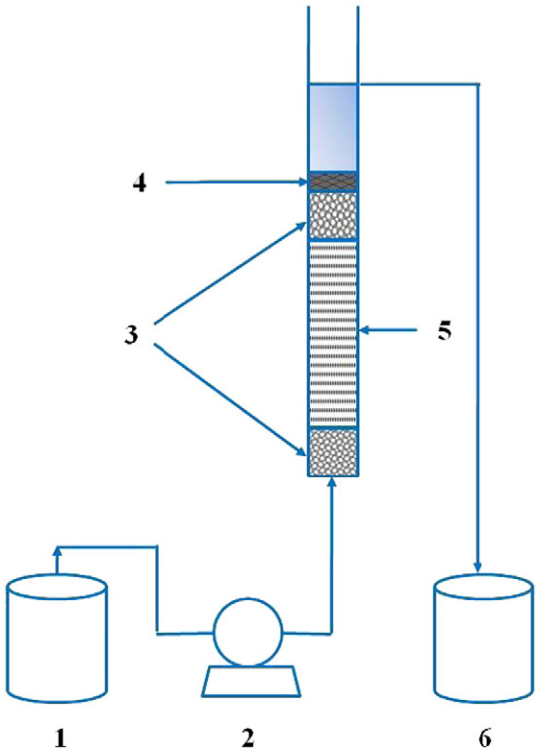

Fig. 1. The schematic diagram of lab-scale mini-column tests (1. Feed tank, 2. Peristaltic pump, 3. Glass beads, 4. Sponge pad, 5. ZLO bed, 6. Effluent storage tank).

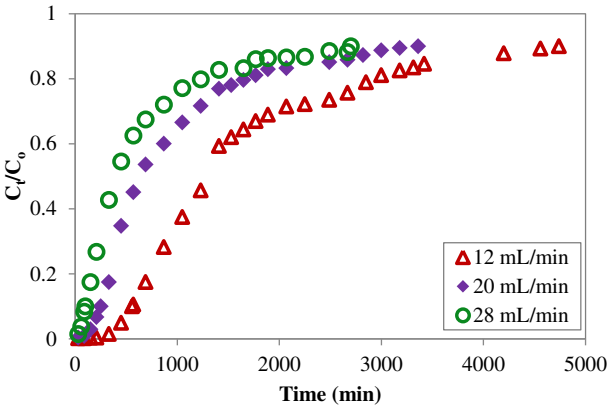

Fig. 2. Effect of flow rate on the breakthrough curve of phosphate adsorption onto ZLO (natural pH, particle size of 1 mm–600 μm, influent phosphorus concentration of 5.5 mg/L, bed height of 23 cm).

The eluted amount of phosphorus (EAP) is calculated by the following equation (Awual and Jyo, 2011):

$$EAP(mg/g) = (1/m) \sum_{q=1}^{n2} C_q V_q \quad (3)$$

where, C_q, V_q, and n2 are the effluent phosphorus concentration, volume of the q-th fraction, and number of the last fraction in the desorption experiment.

The mass transfer zone (MTZ), which is defined as the length of the adsorption zone in the column, can be obtained from the following equation (Bulgariu and Bulgariu, 2013):

$$MTZ = H\frac{(t_s - t_b)}{t_s} \quad (4)$$

where, MTZ represents the length of the mass transfer zone (cm); H is the bed height (cm); t_b is the breakthrough time (min); and t_s is the exhaustion time (min).

The empty bed contact time (EBCT) in the column (min) is achieved from the ratio of bed volume (mL) to the flow rate (mL/min) as follows (Ohura et al., 2011):

$$EBCT = \frac{\text{Bed volume}}{\text{Flow rate}}. \quad (5)$$

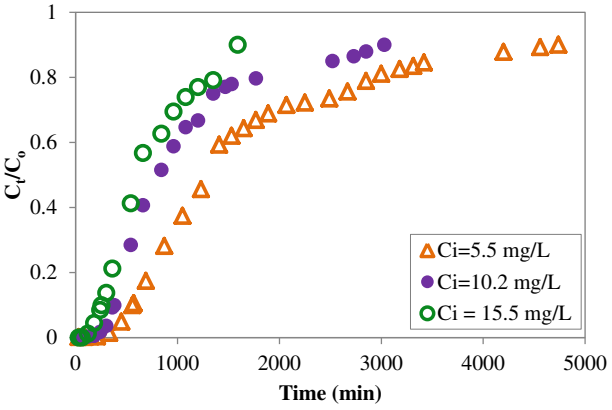

Fig. 3. Effect of influent phosphorus concentration on the breakthrough curve of phosphate adsorption onto ZLO (natural pH, particle size of 1 mm–600 μm, flow rate of 12 mL/min, bed height of 23 cm).

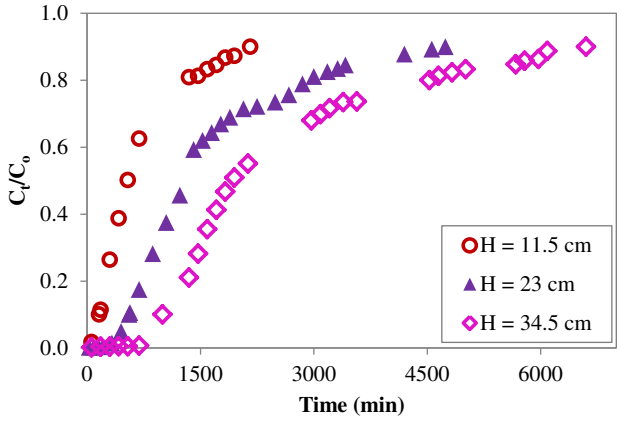

Fig. 4. Effect of bed height on the breakthrough curves of phosphate adsorption onto ZLO (natural pH, particle size of 1 mm–600 μm, flow rate of 12 mL/min, influent phosphorus concentration of 5.5 mg/L).

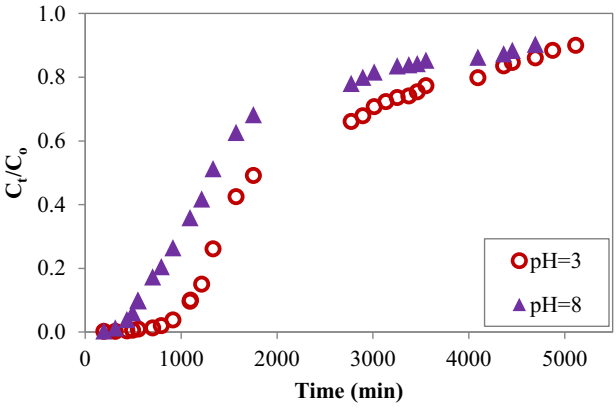

Fig. 5. Effect of pH on the breakthrough curve of phosphate adsorption on ZLO (bed height of 23 cm, flow rate of 12 mL/min, influent phosphorus concentration of 5.6 mg/L, particle size of 1 mm–600 μm).

2.5. Statistical analysis

Experiments were implemented in triplicate, and the data represented the mean values. The highest acceptable deviation was 5%. The error bars indicating the standard deviation were shown in figures wherever possible.

3. Results and discussion

3.1. Removal of phosphate from synthetic solution

3.1.1. Effect of column design parameters

3.1.1.1. Effect of flow rate. The effect of flow rates on phosphorus adsorption by ZLO was explored with various flow rates (12, 20, and 28 mL/min) and a constant bed height (23 cm), initial phosphorus concentration (5.5 mg/L). The breakthrough curves for the column were determined by plotting the C_t/C_o (C_t and C_o are the phosphorus concentration of effluent and influent, respectively) against the time and depicted in Fig. 2. As can be seen from Fig. 2, the shorter breakthrough time occurred at higher flow rate. It can be explained by the fact that larger volume of water elapsed through the bed at higher flow rate. As a consequence, more phosphate ions contacted with the binding sites of ZLO, making them get saturated more quickly. Similarly, higher adsorption capacity was attained at lower flower rate. It is probably because lower flow rate resulted in more residence time of the phosphorus ions in the column. Since phosphate ions had longer contact with ZLO, equilibrium can be reached before phosphate ions moved out of the column (Jain et al., 2013). These findings agree with the previous studies conducted by Awual and Jyo (2011), and Paudyal et al. (2013).

3.1.1.2. Effect of influent phosphorus concentration. It is reported that influent phosphorus concentration can also affect the breakthrough curve (Awual and Jyo, 2011). Fig. 3 illustrated the breakthrough curves for varying feed phosphorus concentrations (5.5, 10.2, and 15.5 mg/L), a given bed height (23 cm) and flow rate (12 mL/min). The breakthrough times were 558, 380, and 254 min for influent phosphorus concentration of 5.5, 10.2, and 15.5 mg/L, respectively. Equally, the exhaustion time declined with a rise in phosphorus initial concentration, from 4740 min (5.5 mg/L) to 3030 min (10.2 mg/L) to 1590 min (15.5 mg/L). It is evident from Fig. 3 that the higher the influent phosphorus concentration was, the faster the breakthrough and exhaustion took place. Higher retention rate and thus, earlier saturation might result from greater concentration gradient and smaller mass transfer resistance at higher phosphate concentration (Mohammed and Rashid, 2012; Paudyal et al., 2013). Similar tendency was reported by Zhang et al. (2014) in case of removing phosphate using activated laterite. The dynamic adsorption capacity of ZLO for phosphorus increased, from 11.93 to 14.28 mg/g with the elevating phosphorus inlet concentration, from 5.5 to 15.5 mg/L. These results are in line with those reported by Awual and Jyo (2011) for the elimination of phosphorus by polymeric anion exchangers.

Table 1
Breakthrough curves parameters for the adsorption of phosphorus onto ZLO at different operating conditions.

pH	Particle size (mm)	Q (mL/min)	H (cm)	C_i (mg/L)	t_b (min)	V_b (L)	q_b (mg/g)	R_b (%)	t_s (min)	V_s (L)	q_s (mg/g)	R_s (%)	m (g/L)	MTZ (cm)
Natural	1–0.6	12	23	5.5	558	6.70	3.59	97.58	4740	56.88	11.93	38.12	1.49	20.29
Natural	1–0.6	20	23	5.5	250	5.00	2.67	96.87	3360	67.20	11.87	32.12	2.00	21.29
Natural	1–.0.6	28	23	5.5	100	2.81	1.48	96.23	2700	75.60	11.84	28.47	3.56	22.15
Natural	1–0.6	12	23	5.5	558	6.70	3.59	97.58	4740	56.88	11.93	38.12	1.49	20.29
Natural	1–0.6	12	23	10.2	380	4.56	4.54	97.74	3030	36.36	14.09	37.99	2.19	20.12
Natural	1–.0.6	12	23	15.5	254	3.05	4.58	97.11	1590	19.08	14.28	48.30	3.28	19.33
Natural	1–0.6	12	11.5	5.5	160	1.92	2.03	95.96	2160	25.92	10.41	36.50	2.60	10.65
Natural	1–0.6	12	23	5.5	558	6.70	3.59	97.58	4740	56.88	11.93	38.12	1.49	20.29
Natural	1–.0.6	12	34.5	5.5	1000	12.00	4.31	97.58	6600	79.20	12.12	41.74	1.25	29.27
Natural	1–0.6	12	11.5	5.5	160.2	1.92	2.03	95.96	2160	25.92	10.41	36.50	2.60	10.65
Natural	0.3–0.15	12	9	5.5	438	5.26	5.68	98.24	3270	39.24	14.97	34.69	0.95	7.79
3	1–0.6	12	23	5.6	1100	13.20	7.25	98.14	5118	61.38	16.43	47.81	0.76	18.05
8	1–0.6	12	23	5.6	550	6.60	3.62	97.85	4698	56.34	12.26	38.86	1.51	20.30

Notation: t_b,V_b — the time and treated volume at 10% breakthrough point; t_s, V_s — the time and treated volume at 90% saturation point; q_b, q_s — the amount of phosphorus captured per unit of dry weight of ZLO at 10% breakthrough point and 90% saturation points, respectively; R_b, R_s — the removal percentage of phosphorus at 10% breakthrough and 90% saturation points, respectively; H — bed height; m — mass of adsorbent per liter; MTZ — mass transfer zone.

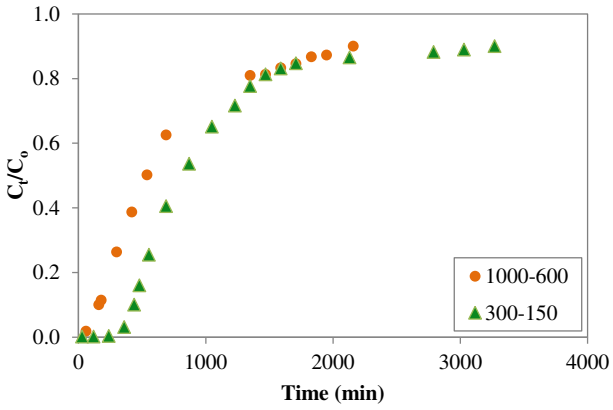

Fig. 6. Effect of particle size on the breakthrough curve of phosphate adsorption onto ZLO (natural pH, bed heights of 11.5 and 9 cm, flow rate of 12 mL/min; influent phosphorus concentration of 5.5 mg/L).

3.1.1.3. Effect of bed height. Fig. 4 described the effect bed height on the breakthrough curve of phosphorus adsorption onto ZLO column. As can be seen from Fig. 4, shorter breakthrough time or steeper breakthrough curve occurred at low bed height. Specifically, the breakthrough time (at C_t/C_o 10%) was 1000, 558, and 160 min for 34.5, 23 and 11.5 cm bed height, respectively. Likewise, the exhaustion time (at C_t/C_o 90%) declined from 6600 to 2160 min when bed height reduced from 34.5 to 11.5 cm. The phosphorus uptake capacity of ZLO was 12.12 and 10.41 mg/g for the bed height of 34.5 and 11.5 cm, respectively as listed in Table 1. The result suggested that reducing bed height led to a fall in phosphorus uptake capacity of ZLO. Jain et al. (2013) attributed this to the less adsorption sites at lower bed height. Conversely, Paudyal et al. (2013) explored that lessening the bed height led to an augmentation of the adsorption capacity of Zr(IV)-DOJR for fluoride. The authors ascribed this to the greater channeling effect at the higher bed depth, and proposed to mitigate this effect by increasing the column diameter.

3.1.1.4. Effect of influent pH. The solution pH is a critical influencing factor to the dynamic adsorption process since it can affect ionic state of the functional groups and phosphate species as well (Chen et al., 2012). The effect of influent pH on phosphate removal by ZLO column was examined at pH values of 3 and 8, while maintaining the same initial phosphorus concentration (5.6 mg/L), bed height (23 cm), and flow rate (12 mL/min). It is clear from Fig. 5 that the breakthrough time increased from 550 to 1099 min with decreasing pH from 8 to 3. It implied that the breakthrough happened more slowly at pH 3. As a result, pH 3 was chosen as the optimal pH for phosphorus adsorption on ZLO column. These findings agreed well with those of the batch adsorption tests reported in the previous paper (Nguyen et al., 2014c). It can be explained by the electrostatic interaction between anionic phosphates species with cationic functional groups on the surface of ZLO. In acidic medium (pH 3), $H_2PO_4^-$ and HPO_4^{2-} species were dominant, which were powerfully retained onto ZLO (Mallampati and Valiyaveettil, 2013). Nevertheless, in alkaline medium (pH 8), the competition between hydroxyl ions with phosphate anions for binding sites led to the decline in phosphate adsorption onto ZLO column. The phosphorus uptake by ZLO packed bed column at pH 3 and pH 8 was 16.43 and 12.26 mg/g, respectively (Table 1). These results are in good agreement with those reported by Awual and Jyo (2011) and Biswas (2008) showing that lower pH can improve phosphate adsorption by a weak-base anion exchange resin named Diaion WA20 and Zr(IV)-loaded SOW gel. Although phosphorus adsorption by ZLO was more efficient at pH 3, in the subsequent experiments, the natural pH of the synthetic solution and municipal wastewater (7.5–8.0) was used to evaluate the actual application of ZLO.

3.1.1.5. Effect of adsorbent particle size. Fig. 6 depicted the effect of adsorbent particle size on the breakthrough curve of phosphate adsorption onto ZLO. It was shown that, the use of smaller ZLO particle size resulted in longer breakthrough time and higher phosphorus uptake capacity. Specifically, as a result of reducing ZLO particle size from 1000–600 to 300–150 μm, the breakthrough occurred more slowly 178 min while the phosphorus uptake capacity boosted by 43.52%. Apparently, the smaller particle size of ZLO facilitates the phosphorus adsorption from aqueous solutions. The larger surface area may be responsible for higher adsorption capacity with smaller particle size. This finding is supported by that of earlier batch adsorption system with ZLO. Similar observation was reported by Okochi (2013) for the removal of phosphorus from stormwater using electric ARC furnace steel slag. Unfortunately, the use of the particle size of 300–150 μm resulted in the column clogging during desorption test with 0.2 M NaOH. To solve this problem, the column should be packed with a mixture of different particle sizes instead of individual particle size. By this way, it is expected to enhance the adsorption capacity of ZLO while reduce the column clogging.

3.1.2. Breakthrough curve modeling

The prediction of the breakthrough curve is essential for designing a continuous adsorption system. The relation between concentration and time provides insights into the adsorbent affinity, adsorbent surface properties, and adsorption pathways (Foo et al., 2013). For that reason, several mathematical models have been developed for this purpose.

Table 2
Adams–Bohart, Thomas and Yoon–Nelson models constants for the phosphorus adsorption by ZLO packed column.

Conditions					Adams–Bohart			Thomas			Yoon–Nelson		
pH	P	Q	Z	C_i	k_{AB}	N_o	R^2	k_{Th}	q_o	R^2	k_{YN}	τ	R^2
Natural	1–0.6	12	23	5.5	109.09	1.26	0.928	0.098	3.29	0.982	0.54	23.95	0.890
Natural	1–0.6	20	23	5.5	200.00	0.99	0.934	0.136	1.75	0.903	0.96	10.62	0.825
Natural	1–.0.6	28	23	5.5	272.73	0.78	0.887	0.140	0.31	0.936	0.99	3.64	0.831
Natural	1–0.6	12	23	5.5	109.09	1.26	0.928	0.098	3.29	0.982	0.54	23.95	0.890
Natural	1–0.6	12	23	10.2	98.04	1.49	0.946	0.099	8.33	0.860	1.21	15.49	0.780
Natural	1–.0.6	12	23	15.5	83.87	1.71	0.790	0.129	12.21	0.963	2.00	10.94	0.963
Natural	1–0.6	12	11.5	5.5	127.00	1.34	0.871	0.182	2.42	0.984	1.00	7.77	0.971
Natural	1–0.6	12	23	5.5	90.91	1.52	0.928	0.098	3.29	0.982	0.54	23.95	0.890
Natural	1–.0.6	12	34.5	5.5	54.55	1.74	0.962	0.076	5.74	0.970	0.49	31.07	0.945
Natural	1–0.6	12	11.5	5.5	109.09	1.44	0.843	0.182	2.42	0.984	1.00	7.77	0.971
Natural	0.3–0.15	12	9	5.5	181.82	2.23	0.945	0.180	7.26	0.742	1.15	13.29	0.730
3	1–0.6	12	23	5.6	71.43	2.18	0.973	0.109	11.00	0.988	0.63	28.28	0.991
8	1–0.6	12	23	5.6	71.42	1.60	0.831	0.100	4.06	0.941	0.75	22.77	0.902

Notation:
P, particle size (mm); Q, feed flow rate (mL/min); Z, bed height (cm); C_i, initial phosphorus concentration (mg/L); k_{AB}, Adams–Bohart model rate constant (L/mg min) × 10^{-5}; N_o, saturation concentration (mg/L) × 10^3; k_{Th}, Thomas model rate constant (mL/mg min) × 10^{-3}; q_o, equilibrium phosphorus sorption capacity (mg/g); k_{YN}, Yoon–Nelson model rate constant (1/min) × 10^{-3}; τ, the time required for 50% breakthrough (min).

This study investigates the dynamic adsorption behavior of ZLO using Adams–Bohart, Thomas, Yoon–Nelson, and BDST models.

3.1.2.1. Adams–Bohart model. Adams–Bohart model assumes that equilibrium is not instant, and the adsorption rate is controlled by external mass transfer (Quintelas et al., 2013). This model is appropriate for analyzing the initial part of the breakthrough curve ($C_t/C_o = 0–0.5$) (Long et al., 2014; Sharma and Singh, 2013). The equation of Adams–Bohart model is expressed as follows:

$$\ln\frac{C_t}{C_0} = K_{AB}\,C_0 t - K_{AB}\,N_0\frac{Z}{F} \tag{6}$$

where C_o and C_t (mg/L) are the influent and effluent phosphorus concentration, K_{AB} (L/mg min) is the kinetic constant, N_o (mg/L) is saturation concentration of the column, Z (cm) is the bed depth, F (cm/min) is the linear velocity achieved by dividing the flow rate (cm^3/min) by the column section area (cm^2).

The constants K_{AB} and N_o of the Adams–Bohart model can be estimated from the linear plot of $\ln(C_t/C_o)$ against t. As seen in Table 2, the adsorption capacity of the bed (N_o) decreased from 1.26 to 0.78 mg/L with increasing flow rate (Q) from 12 to 28 mL/min. Conversely, N_o value expanded from 1.34 to 1.74 mg/L when bed height rose from 11.5 to 34.5 cm. The increase in initial phosphorus concentration from 5.5 to 15.5 mg/L led to a growth in N_o value, from 1.26 to 1.71 mg/L. The kinetic constant (k_{AB}) declined from 127 to 54.55 L/(mg min) with increasing bed height (Z) from 11.5 to 34.5 cm. On the contrary, the k_{AB} value extended from 109.09 to 272.73 L/(mg min) with growing flow rate (Q) from 12 to 28 mL/min. The results suggest that, better adsorption performance of the column, characterized by higher adsorption capacity (N_o) and lower kinetic constant (k_{AB}), can be achieved with higher initial phosphorus concentration (C_o) and bed height (Z), but lower feed flow rate (Q) (Bulgariu and Bulgariu, 2013). The correlation coefficients obtained with Adams–Bohart model were higher than 0.9 in a large proportion (8/13) of the adsorption tests. It indicates that Adams–Bohart model can provide a relatively good fit to the phosphorus-ZLO adsorption system.

3.1.2.2. Thomas model. Thomas model is developed on the assumption that (1) the adsorption is not limited by chemical interactions but by mass transfer at the interface and (2) the experimental data follows Langmuir isotherms and second-order kinetics (Foo et al., 2013). Unlike Adams–Bohart model, Thomas model is appropriate for depicting the whole breakthrough curve (Bulgariu and Bulgariu, 2013). Thomas model can be written in the linear form by the following equation (Paudyal et al., 2013):

$$\ln\left(\frac{C_0}{C_t}-1\right) = k_{Th}\,q_o\frac{m}{Q} - k_{Th}C_0 t \tag{7}$$

where k_{Th} stands for Thomas rate constant (mL/min mg), q_o is the adsorption capacity (mg/g), C_o is the inlet phosphorus concentration (mg/L), C_t is the outlet phosphorus concentration at time t (mg/L), m is the mass of adsorbent (g), Q is the feed flow rate (mL/min), and t is the filtration time (min). The values of k_{Th} and q_o were determined from the linear plot of $\ln\left(\frac{C_0}{C_t}-1\right)$ against t and shown in Table 2.

As the flow rate increased (12 to 28 mL/min), the Thomas rate constant increased (0.098 to 0.140 mL/(min mg)), whereas the adsorption capacity reduced (3.29 to 0.31 mg/g). An increase in initial phosphorus concentration (5.5 to 15.5 mg/L) led to an elevation in both Thomas rate constant (0.098 to 0.129 mL/(min mg)) and adsorption capacity (3.29 to 12.21 mg/g). The increase in bed depth (11.5 to 34.5 cm) resulted in a decrease in the Thomas rate constant (0.182 to 0.076 mL/(min mg)), but a growth in uptake capacity (2.42 to 5.74 mg/g). Superior uptake capacity at the higher feed phosphorus concentration can be attributed to the larger concentration gradient and higher driving force (Paudyal et al., 2013). Similar trend was reported by Bulgariu and Bulgariu (2013), Long et al. (2014) and Samuel et al. (2013). In a majority of the adsorption tests (11/13), the correlation coefficients of Thomas models were above 0.9. It validates the applicability of Thomas model to the phosphorus-ZLO adsorption system. Also, the adsorption process was not regulated by internal and external diffusions (Chen et al., 2012).

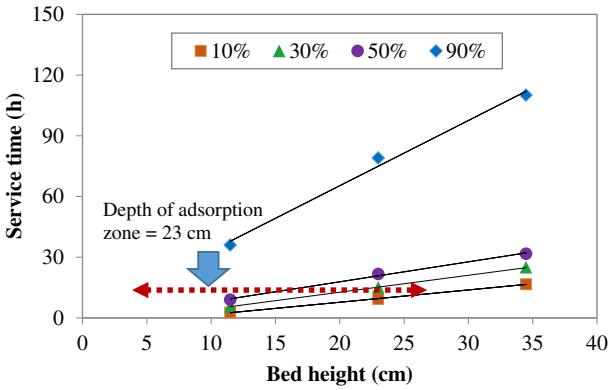

Fig. 7. BDST model for 10%, 30%, 50%, and 90% breakthrough at different bed depths and constant inlet phosphorus concentration (5.5 mg/L) and flow rate (12 mL/min).

3.1.2.3. Yoon–Nelson model. Similar to Thomas model, Yoon–Nelson model can mitigate limitations of Adams–Bohart model at later period of the breakthrough curve. The linear expression of Yoon–Nelson model is given by the following equation (Sharma and Singh, 2013):

$$\ln\left(\frac{C_t}{C_0-C_t}\right) = k_{YN}t - \tau k_{YN} \tag{8}$$

where k_{YN} is the Yoon–Nelson rate constant (min^{-1}), and τ is the time required for 50% phosphorus breakthrough (min).

Table 2 represents Yoon–Nelson model parameters (k_{YN} and τ) which were calculated from the linear plot of $\ln[C_t/(C_o - C_t)]$ against t. It was found that k_{YN} increased (0.54 to 0.99 min^{-1}) while τ decreased (23.95 to 3.64 h) with an increase in the flow rate (12 to 18 mL/min). Similar trend occurred to k_{YN} and τ with the increasing influent phosphorus concentration. Sharma and Singh (2013) explained these results by the faster saturation of the column at higher flow rate and inlet phosphorus concentration. Nevertheless, τ was extended at higher bed depths. Similar trends were reported by Chen et al. (2012) and Long et al. (2014). The τ values predicted by Yoon–Nelson model were quite similar to those obtained from experiments. Nevertheless, in the most cases (7/13), Yoon–Nelson model resulted in the correlation coefficients below 0.9. It demonstrated that Yoon–Nelson model was less satisfactory than Adams–Bohart model and Thomas model in describing the phosphate-ZLO adsorption system.

3.1.2.4. BDST model. The BDST model is to represent the relationship between bed depth and service time. It is reported that BDST model can describe appropriately initial part (10–50%) of the breakthrough curve (Jain et al., 2013). The linear expression of BDST model is given by the

Table 3
BDST model constants for adsorption of phosphorus on ZLO.

Breakpoint (%)	m (h/cm)	C (h)	N_o (mg/L)	K_b (L/mg h)	Z_o (cm)	R^2
10	0.608	−4.555	16.69	0.0897	7.33	0.999
30	0.840	−4.106	23.06	0.0973	4.89	0.999
50	0.985	−1.89	27.04	0.2114	1.92	0.995

Table 4
Prediction of the breakthrough time for various bed depths by BDST model.

Bed depth (cm)	10% breakthrough		50% breakthrough	
	Predicted t_b (h)	Observed t_b (h)	Predicted t_b (h)	Observed t_b (h)
11.5	2.44	2.67	9.44	9.00
23	9.43	9.30	20.77	21.67
34.5	16.42	16.67	32.09	32.50

following equation (Li et al., 2013; Paudyal et al., 2013):

$$t = \frac{ZN_o}{C_o v} - \frac{1}{K_b C_o} \ln\left(\frac{C_o}{C_b} - 1\right) \quad (9)$$

where t is the service time of column (h), Z is the bed depth (cm), C_o is the inlet phosphorus concentration (mg/L), C_b is the outlet concentration at breakthrough point (mg/L), N_o is the column adsorption capacity (mg/L), K_b is the rate constant [L/(mg h)], and v is the linear flow velocity and is calculated by dividing the flow rate by the area of column (cm/min).

From the plots of time versus bed depth (Fig. 7), the BDST parameters, namely N_o and K_b, are calculated as follows (Zach-Maor et al., 2011):

$$m = \text{slope} = \frac{N_o}{C_o v} \rightarrow N_o = mC_o v \quad (10)$$

$$C = \text{intercept} = -\frac{1}{K_b C_o} \ln\left(\frac{C_o}{C_b} - 1\right) \rightarrow K_b = -\frac{1}{C * C_o} \ln\left(\frac{C_o}{C_b} - 1\right). \quad (11)$$

Setting t = 0 and solving Eq. (9) for Z produces the following equation (Kumar and Bandyopadhyay, 2006):

$$Z_o = \frac{v}{K_b N_o} \ln\left(\frac{C_o}{C_b} - 1\right) \quad (12)$$

where Z_o (cm) is called the critical bed depth, which is the minimum bed depth required to yield the desired effluent concentration (C_b).

Table 3 represents BDST model constants (N_o, K_b) and corresponding critical bed depth (Z_o) for various breakthrough points (10%, 30%, and 50%) at constant initial phosphorus concentration (5.5 mg/L) and flow rate (12 mL/min). The high correlation coefficients ($R^2 > 0.995$) demonstrated that BDST model could efficiently depict the phosphate–ZLO dynamic adsorption system.

The adsorption zone, known as mass transfer zone (MTZ), can be defined as the adsorbent layer through which the effluent concentration changes from 10 to 90% of the influent concentration. MTZ is identified as the horizontal distance between these two lines in the BDST plot (Kumar and Bandyopadhyay, 2006). From Fig. 7, MTZ in this study was estimated to be 23 cm. The Eq. (9) allows predicting the breakthrough time (t_b) for a new bed depth (Z) without conducting further experiments. The prediction utilizes N_o, K_b values determined at the same initial phosphorus concentration (C_o) and velocity (v). Table 4 represents the predicted and observed breakthrough times for varying bed depths. It was found that the breakthrough times calculated by BDST model were quite similar to those obtained from the experiment. It validates the applicability of BDST model to phosphorus–ZLO dynamic adsorption system.

3.1.3. Dynamic adsorption capacity of ZLO

The dynamic adsorption capacity of ZLO for phosphorus at the breakthrough time and exhaustion time was calculated for different operating conditions and summarized in Table 1. The highest adsorption capacity of ZLO at the exhaustion time was 16.43 mg/g, accounting for 85.44% its equilibrium adsorption capacity. This maximum value was achieved for a bed height of 23 cm, flow rate of 12 mL/min and initial phosphorus concentration of 5.6 mg/L, particle size of 1000–600 μm, and influent pH of 3.

Table 5 summarizes the dynamic phosphorus adsorption capacity of ZLO in this study and various adsorbents in the literature. It was shown that, ZLO was favorably comparable to most of the reported adsorbents. The result indicated that ZLO can effectively remove phosphorus in the continuous adsorption systems. The reasonably high adsorption capacity of ZLO column for phosphorus can be explained by the fact that Zr(IV) loading resulted in the development of effective binding sites for phosphate anions on the surface of okara. Consequently, the retention of phosphate onto ZLO was strengthened.

3.2. Application of ZLO packed bed column in treating real municipal wastewater

3.2.1. Comparative study on phosphate adsorption by ZLO with synthetic solution and real municipal wastewater

The application of ZLO in treating real wastewater was tested in a mini-column using the sewage secondary effluent, which was collected from Sydney Olympic Park Water Treatment Plant. The sewage composition was determined as follows: pH 7.68, salinity 0.42‰, turbidity 87.9 NTUs, electrical conductivity 870 μS/cm, total suspended solids (TSS) 84 mg/L, ammonium (NH_4–N) 51 mg/L, nitrate (NO_3^-–N) 3.60 mg/L, nitrite (NO_2^-–N) 0.19 mg/L, orthophosphate (PO_4–P) 5.7 mg/L, total organic carbon (TOC) 22.05 mg/L, chemical oxygen demand (COD)

Table 5
Comparison of the dynamic adsorption capacity for phosphorus of ZLO with various adsorbents.

Adsorbent	Z (cm)	Q (mL/min)	C_i (mg/L)	pH	Temp. (°C)	q_b (mg/g)	q_s (mg/g)	Reference
Diaion WA20	–	1.67	34.68	7	–	12.74	–	Awual and Jyo (2011)
La(III)-loaded SOW	–	0.12	20	7.5	30	–	13.63	Biswas et al. (2007)
Zr(IV)-loaded SOW	–	–	20	7	30		10	Biswas (2008)
Zr(IV)-loaded SOW	–	–	20	3	30		36	Biswas (2008)
CP-Fe-I	–	6.1	16.32	–	30	–	22.19	Krishnan and Haridas (2008)
Purolite FerrIX A33E	19	13	20	7.2–7.6	Room	12.5	–	Nur et al. (2014)
Purolite FerrIX A33E	12	13	5	7.2–7.6	Room	4.1	–	Nur et al. (2014)
Zr(IV)-loaded SOW	–	0.20	5.9		30	–	40.3	Ohura et al. (2011)
Steel slag	7.5	7.92	–	6.0–7.4	Room	–	0.7	Okochi (2013)
AC-WS	–	5	100	–	–	–	13.67	Xu et al. (2011a)
AC-CS	–	5	100	–	–	–	16.01	Xu et al. (2011a)
GR based resin	–	5	200	5.12	–	–	17.84	Xu et al. (2011b)
Zr(IV)-loaded okara	23	12	5.6	3	Room	7.25	16.43	This study
Zr(IV)-loaded okara	9	12	5.5	7.6	Room	5.68	14.97	This study

Notation:
Z, bed depth (cm); Q, flow rate (mL/min); C_i, influent phosphorus concentration (mg/L); q_b, column adsorption capacity at breakthrough time (mg/g), q_s, column adsorption capacity at exhaustion time (mg/g).

239 mg/L, chloride (Cl^-) 108.10 mg/L, calcium (Ca^{2+}) 30.55 mg/L, magnesium (Mg^{2+}) 9.2 mg/L, iron (Fe^{2+}) 0.25 mg/L, copper (Cu^{2+}) 0.1 mg/L, lead (Pb^{2+}) 0.35 mg/L, manganese (Mn^{2+}) 0.04 mg/L, nickel (Ni^{2+}) 0.02 mg/L, zinc and cadmium cannot be detected. Obviously, the concentration of heavy metals was negligible in municipal wastewater. The sewage was settled for 24 h prior to adsorption test. Fig. 8 shows the breakthroughs for phosphorus adsorption onto ZLO column using synthetic solution and real municipal wastewater for comparison purpose. It was found that the phosphorus level of the sewage was lowered to the recommended discharge limit (1 mg/L) for a period of 210 min, using a column packed with only 10 g of ZLO. Comparing the phosphorus content of the sewage before and after passing through ZLO column showed that more than 90% phosphorus was eliminated from 5880 mL sewage in 210 min. The results proved that phosphorus from the sewage was successfully captured by ZLO column. The breakthrough time and the dynamic adsorption capacity of ZLO obtained with the sewage were quite similar to those with the synthetic solution. The results indicated that the effect of co-existing ions in the sewage on the continuous adsorption process was negligible. As a final remark, ZLO is capable of removing phosphorus from the real municipal wastewater in the dynamic adsorption system.

3.2.2. Successive adsorption–desorption cycles

3.2.2.1. Adsorption of phosphate onto ZLO packed bed column. In order to investigate the reusability of ZLO in the reality, the adsorption tests of ZLO were repeated three times with real municipal wastewater. Fig. 9 represents the breakthrough curves for three adsorption times of ZLO. It is clear from Fig. 9 that there was no big difference among breakthrough curves for three adsorption times. For the first time, the breakthrough occurred at 60 min while the exhaustion achieved at 1500 min. For the third time, the breakthrough time and exhaustion time were 90 min and 1710 min, respectively. Despite a slight reduction in the adsorption capacity (18.64%) and removal percentage at the exhaustion time (7.30%) after three adsorption times, the regenerated ZLO still had a high adsorption capacity, and thus it can be kept recycling.

3.2.2.2. Elution of loaded phosphorus and regeneration of exhausted ZLO. Desorption and regeneration play a critical role in sustainable use of the adsorbent (Jain et al., 2013; Xu et al., 2011b). In the earlier batch adsorption tests, the dilute alkaline solution (0.2 M NaOH) was proven to be the best desorption solution (Nguyen et al., 2014b). In the present study, 0.2 M NaOH was employed for eluting phosphorus from saturated ZLO column. Prior to desorption test, phosphorus saturated ZLO column was washed with an abundant amount of distilled water to eliminate unbound phosphate ions. In the first cycle, more than 70% of

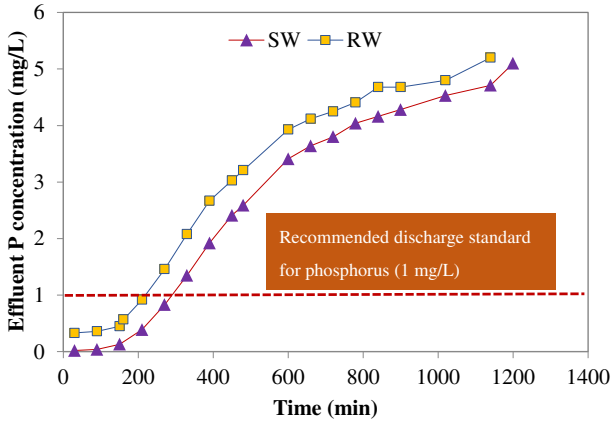

Fig. 8. Breakthrough curves for phosphorus adsorption from synthetic and real municipal wastewater by ZLO (Particle size > 600 μm; bed depth 21 cm, flow rate 28 mL/min, inlet phosphorus concentration 5.7 mg/L).

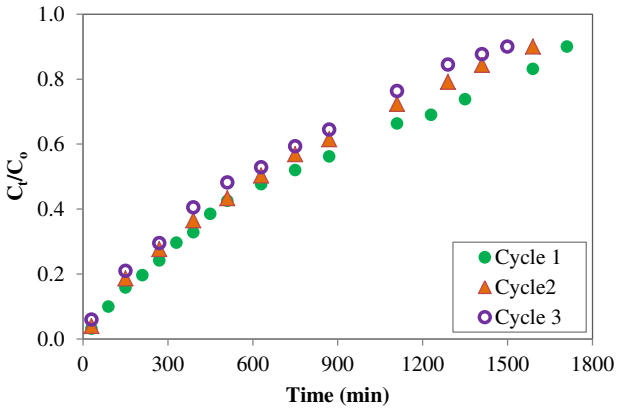

Fig. 9. Breakthrough curves for phosphorus adsorption from municipal wastewater by ZLO in three cycles (influent phosphorus concentration of 6.0 mg/L, flow rate of 12 mL/min, bed depth of 10 cm, and particle size of 1 mm–600 μm).

loaded phosphorus was eluted when 360 mL of 0.2 M NaOH was percolated through the column, which lasted for around 0.5 h. The effluent phosphorus concentration at 0.5 h was 112 mg/L, 18.67 times higher than the feed phosphorus concentration. Desorption process was almost completed within 2.75 h with the efficiency reached up to 92.16%, indicating that the adsorption of phosphorus onto ZLO column was revisable. After three cycles of operation, the desorption efficiency of ZLO column was still above 88% (Table 6), showing that ZLO column had excellent regeneration property. The elution of phosphate from ZLO column might result from ion exchange reaction, whereby OH^- ions from NaOH displaced phosphate ions from ZLO surface. Nevertheless, after three cycles of adsorption–desorption, the weight loss of ZLO column was found to be 8.7%. This is in line with the result by Xu et al. (2011b), who reported that the weight loss after three adsorption–desorption cycles of the cotton stalk and wheat stalk was about 5%. The authors suggested this weight loss might result from the corrosion of cellulose and hemicelluloses in these adsorbents, caused by HCl desorption solution. After several cycles of operation, ZLO may be lack of efficiency to separate phosphorus from wastewater. By that time, it was recommended to recover loaded Zr(IV) using acids (e.g., 0.5 M HCl) while recycle the residual substrate as fertilizer (Paudyal et al., 2013).

3.2.3. Effect of ZLO packed bed column on the effluent quality

Table 7 describes the sewage properties before and after passing through the ZLO column. ZLO removed more than 90% phosphate but only around 50% nitrate and 0% nitrite. It would seem that though ZLO adsorbed several anions, the highest affinity was shown to phosphate. Regarding the cationic ions, ZLO eliminated ammonium (NH_4^+), magnesium (Mg^{2+}), calcium (Ca^{2+}) and iron (Fe^{2+}) with the efficacy of 18.63, 30.98, 53.19, and 40%, respectively. The result proved that ZLO had a potential of reducing the hardness from municipal wastewater. In contrast, ZLO could hardly remove common heavy metals, such as Cu(II) and Pb(II). It can be interpreted that the binding sites provided by ZLO were more appropriate for anionic adsorption. In view of phosphorus recovery, this can be regarded as an advantageous feature of ZLO as it helps improve the purity of phosphorus recovered products. Zr(IV) could not be detected in the effluent, implying that no Zr(IV) was

Table 6
Phosphorus adsorption–desorption parameters for three cycles of adsorption–desorption with real municipal wastewater.

Cycle no	Breakthrough time (min)	Exhaustion time (min)	Exhaustion uptake (mg/g)	Desorption efficiency (%)
1	90	1710	11.64	92.16
2	75	1590	10.34	89.33
3	60	1500	9.47	88.54

Table 7
Characteristics of municipal wastewater before and after passing through ZLO packed bed column (influent phosphorus concentration of 5.7 mg/L, flow rate of 28 mL/min, bed height of 21 cm, and particle size of 1 mm–600 μm).

Quality parameter	Initial municipal wastewater	Treated municipal wastewater	Maximum permissible level[a]	Maximum permissible level[b]
Phosphate (PO_4–P), mg/L	5.70	0.57	1.0	–
Nitrate (NO_3–N), mg/L	3.60	1.80	20	37
Nitrite (NO_2–N), mg/L	0.19	0.19	–	–
Chloride, mg/L	108.10	147.13	–	500
Ammonia (NH_4–N), mg/L	51	41.5	–	–
Mg(II), mg/L	9.20	6.35	–	100.60
Ca(II), mg/L	30.55	14.3	–	300
Cu(II), mg/L	0.1	0.1	0.5	–
Zn(II), mg/L	Not detected	Not detected	1.5	–
Pb(II), mg/L	0.35	0.35	0.20	0.20
Cd(II), mg/L	Not detected	Not detected	0.05	–
Zr(IV), mg/L	Not detected	Not detected	–	–
Fe(II), mg/L	0.25	0.15	–	–
TOC, mg/L	55.88	74.32	–	–
COD, mg/L	239	315	500	–

Notation:
[a] According to the National Standards of PRC (GB 21900–2008) (Long et al., 2014).
[b] According to Romanian legislation (NTPA 001/2005) (Bulgariu and Bulgariu, 2013).

detached during the adsorption process. It is worth noting that the chloride ions, TOC, and COD levels increased markedly after the column treatment. The results indicated that some chloride and organic matters might be released from ZLO into the solution during the adsorption performance. However, the values of these parameters in the effluent were still lower than the permission levels, especially for chloride. This can be considered as side-effects of using biomaterials derived adsorbents. Similar observation was reported by Bulgariu and Bulgariu (2013). Generally, the quality of municipal sewage was improved by the treatment with ZLO packed bed column. The high content of organic matter in the effluent will be beneficial provided that the ZLO column treatment is installed as the earlier stage of BOD and nitrogen removal, whereby carbon sources are often required.

4. Conclusion

This study explores that ZLO can efficiently remove phosphorus from water and wastewater in the column mode. The adsorption performance of the column was influenced by influent pH, initial phosphorus concentration, bed height, flow rate, and adsorbent particle size. The highest dynamic adsorption capacity of ZLO for phosphorus was 16.43 mg/g. Both the BDST and Thomas model fitted well the experimental data. 92.16% loaded phosphorus could be desorbed by 0.2 M NaOH. ZLO could repeatedly be used for at least three cycles with a minor reduction in the uptake capacity and a marginal weight loss. Effluent standard for phosphorus in Australia was achieved from municipal wastewater by using ZLO column. Although Zr(IV) leakage was not found, some organic matters and chloride were released from ZLO into the solution during its performance.

Acknowledgments

The main author gratefully thanks the Australia Awards for providing her with a full scholarship. We would like to acknowledge the Centre for Technology in Water and Wastewater (CTWW), School of Civil and Environmental Engineering, University of Technology, Sydney (UTS) for the financial support. We thank Lijuan Deng, a PhD candidate at UTS, for providing valuable helps to take care of our experiments at nights.

References

Ackerman, J.N., 2012. Reclaiming phosphorus as struvite from hog manure. (Doctoral thesis). University of Manitoba, Winnipeg, Canada.
Awual, M.R., Jyo, A., 2011. Assessing of phosphorus removal by polymeric anion exchangers. Desalination 281, 111–117.
Biswas, B.K., 2008. Removal and recovery of arsenic and phosphorus by means of adsorption onto orange waste, an available agricultural by-product. (Doctoral thesis). Saga University, Saga, Japan.
Biswas, B.K., Inoue, K., Ghimire, K.N., Ohta, S., Harada, H., Ohto, K., et al., 2007. The adsorption of phosphate from an aquatic environment using metal-loaded orange waste. J. Colloid Interface Sci. 312, 214–223.
Bottini, A., Rizzo, L., 2012. Phosphorus recovery from urban wastewater treatment plant sludge liquor by ion exchange. Sep. Sci. Technol. 47, 613–620.
Bulgariu, D., Bulgariu, L., 2013. Sorption of Pb(II) onto a mixture of algae waste biomass and anion exchanger resin in a packed bed column. Bioresour. Technol. 129, 374–380.
Carvalho, W.S., Martins, D.F., Gomes, F.R., Leite, I.R., Gustavo da Silva, L., Ruggiero, R., et al., 2011. Phosphate adsorption on chemically modified sugarcane bagasse fibres. Biomass Bioenergy 35, 3913–3919.
Chen, S., Yue, Q., Gao, B., Li, Q., Xu, X., Fu, K., 2012. Adsorption of hexavalent chromium from aqueous solution by modified corn stalk: a fixed bed column study. Bioresour. Technol. 113, 114–120.
Eberhardt, T.L., Min, S.H., 2008. Biosorbents prepared from wood particles treated with anionic polymer and iron salt: effect of particle size on phosphate adsorption. Bioresour. Technol. 99, 626–630.
Foo, K.Y., Lee, L.K., Hameed, B.H., 2013. Preparation of tamarind fruit seed activated carbon by microwave heating for the adsorptive treatment of landfill leachate: a laboratory column evaluation. Bioresour. Technol. 133, 599–605.
Greenlee, L.F., Lawler, D.F., Freeman, B.D., Marrot, B., Moulin, P., 2009. Reverse osmosis desalination: water sources, technology, and today's challenge. Water Res. 43, 2317–2348.
Jain, M., Garg, V.K., Kadirvelu, K., 2013. Cadmium(II) sorption and desorption in a fixed bed column using sunflower waste carbon calcium-alginate beads. Bioresour. Technol. 129, 242–248.
Jia, G., 2014. Nutrient Removal and Recovery by the Precipitation of Magnesium Ammonium Phosphate. (Master of Science thesis). The University of Adelaide, South Australia, Australia.
Kalmykova, Y., Fedje, K., 2013. Phosphorus recovery from municipal solid waste incineration fly ash. Waste Manag. 33, 1403–1410.
Krishnan, K.A., Haridas, A., 2008. Removal of phosphate from aqueous solutions and sewage using natural and surface modified coir pith. J. Hazard. Mater. 152, 527–535.
Kumar, U., Bandyopadhyay, M., 2006. Fixed bed column study for Cd(II) removal from wastewater using treated rice husk. J. Hazard. Mater. B129, 253–259.
Kumar, R., Bhatia, D., Sigh, R., Rani, S., Bishnoi, N.R., 2011. Sorption of heavy metals from electroplating effluent using immobilized biomass *Trichodermaviride* in a continuous packed-bed column. Int. Biodeterior. Biodegrad. 65, 1133–1139.
Li, N., Ren, J., Zhao, L., Wang, Z., 2013. Fixed bed adsorption study on phosphate removal using nanosized FeOOH-modified anion resin. J. Nanomater. volume 2013. http://dx.doi.org/10.1155/2013/736275 (Article ID 736275, 5 pages).
Long, Y., Lei, D., Ni, J., Ren, Z., Chen, C., Xu, H., 2014. Packed bed column studies on lead(II) removal from industrial wastewater by modified *Agaricusbisporus*. Bioresour. Technol. 152, 457–463.
Mallampati, R., Valiyaveettil, S., 2013. Apple peel — a versatile biomass for water purification. ACS Appl. Mater. Interfaces 5, 4443–4449.
Martín, M., Gargallo, S., Hernández-Crespo, C., Oliver, N., 2013. Phosphorus and nitrogen removal from tertiary treated urban wastewaters by a vertical flow constructed wetland. Ecol. Eng. 61, 34–42.
Mohammed, W.T., Rashid, S.A., 2012. Phosphorus removal from wastewater using oven dried alum sludge. Int. J. Chem. Eng. volume 2012. http://dx.doi.org/10.1155/2012/125296 (Article ID 125296, 11 pages).
Nguyen, T.A.H., Ngo, H.H., Guo, W.S., Zhang, J., Liang, S., Lee, D.J., 2014a. Modification of agricultural waste/by-products for enhanced phosphate removal and recovery: potential and obstacles. Bioresour. Technol. 169, 750–762.
Nguyen, T.A.H., Ngo, H.H., Guo, W.S., Nguyen, T.V., Zhang, J., Liang, S., et al., 2014b. A comparative study on different metal loaded soybean milk by-product 'okara' for biosorption of phosphorus from aqueous solution. Bioresour. Technol. 169, 291–298.

Nguyen, T.A.H., Ngo, H.H., Guo, W.S., Zhou, J.L., Wang, J., Liang, H., et al., 2014c. Phosphorus elimination from aqueous solution using 'zirconium loaded okara' as a biosorbent. Bioresour. Technol. 170, 30–37.

Nur, T., Johir, M.A.H., Loganathan, P., Vigneswaran, S., Kandasamy, J., 2014. Phosphate removal from water using an iron oxide impregnated strong base anion exchange resin. J. Ind. Eng. Chem. 20, 1301–1307.

Ohura, S., Harada, H., Biswas, B.K., Kondo, M., Ishikawa, S., Kawakita, H., et al., 2011. Phosphorus recovery from secondary effluent and side-stream liquid in a sewage treatment plant using zirconium-loaded saponified orange waste. J. Mater. Cycles Waste Manag. 13, 293–297.

Okochi, N.C., 2013. Phosphorus Removal From Stormwater Using Electric ARC Furnace Steel Slag. (Doctoral thesis). University of Regina, Regina, Canada.

Paudyal, H., Pangeni, B., Inoue, K., Kawakita, H., Ohto, K., Alam, S., 2013. Adsorptive removal of fluoride from aqueous medium using a fixed bed column packed with Zr(IV) loaded dried orange juice residue. Bioresour. Technol. 146, 713–720.

Quintelas, C., Pereira, R., Kaplan, E., Tavares, T., 2013. Removal of Ni(II) from aqueous solutions by an Arthrobacterviscosus biofilm supported on zeolite: from laboratory to pilot scale. Bioresour. Technol. 142, 368–374.

Ren, Z., Shao, L., Zhang, G., 2012. Adsorption of phosphate from aqueous solution using an iron–zirconium binary oxide sorbent. Water Air Soil Pollut. 223, 4221–4231. http://dx.doi.org/10.1007/s11270-012-1186-5.

Samuel, J., Pulimi, M., Paul, M.L., Maurya, A., Chandrasekaran, N., 2013. Batch and continuous flow studies of adsorptive removal of Cr(VI) by adapted bacterial consortia immobilized in alginate beads. Bioresour. Technol. 128, 423–430.

Sharma, R., Singh, B., 2013. Removal of Ni(II) ions from aqueous solutions using modified rice straw in a fixed bed column. Bioresour. Technol. 146, 519–524.

Xu, X., Gao, Y., Gao, B., Tan, X., Zhao, Y.Q., Yue, Q., et al., 2011a. Characteristics of diethylenetriamine-crosslinked cotton stalk, wheat stalk and their biosorption capacities for phosphate. J. Hazard. Mater. 192, 1690–1696.

Xu, X., Gao, B., Yue, Q., Zhong, Q., 2011b. Sorption of phosphate onto giant reed based adsorbent: FTIR, Raman spectrum analysis and dynamic sorption/desorption properties in filter bed. Bioresour. Technol. 102, 5278–5282.

Zach-Maor, A., Semiat, R., Shemer, H., 2011. Fixed bed phosphate adsorption by immobilized nano-magnetite matrix: experimental and a new modelling approach. Adsorption 17, 929–936.

Zhang, L., Wu, W., Liu, J., Zhou, Q., Luo, J., Zhang, J., et al., 2014. Removal of phosphate from water using raw and activated laterite: batch and column studies. Desalin. Water Treat. 52, 775–783.